

Selection of design and operational parameters in spindle–holder–tool assemblies for maximum chatter stability by using a new analytical model

A. Ertürk^a, E. Budak^b, H.N. Özgüven^{a,*}

^aDepartment of Mechanical Engineering, Middle East Technical University, 06531 Ankara, Turkey

^bFaculty of Engineering and Natural Sciences, Sabanci University, Orhanli, Tuzla, 34956 Istanbul, Turkey

Received 29 June 2006; received in revised form 27 July 2006; accepted 24 August 2006

Available online 10 October 2006

Abstract

In this paper, using the analytical model developed by the authors, the effects of certain system design and operational parameters on the tool point FRF, thus on the chatter stability are studied. Important conclusions are derived regarding the selection of the system parameters at the stage of machine tool design and during a practical application in order to increase chatter stability. It is demonstrated that the stability diagram for an application can be modified in a predictable manner in order to maximize the chatter-free material removal rate by selecting favorable system parameters using the analytical model developed. The predictions of the model, which are based on the methodology proposed in this study, are also experimentally verified.

© 2006 Elsevier Ltd. All rights reserved.

Keywords: Chatter stability; Machine tool dynamics; Spindle dynamics; Tool point FRF

1. Introduction

Self-excited vibrations of the tool result in unstable cutting process, poor surface finish, reduced productivity and damage on the machine tool itself. For the last 50 years, several important studies have been conducted for predicting regenerative chatter and preventing unstable cutting [1–5]. Today, it is possible to obtain stable (chatter-free) spindle speed and depth of cut combinations by using the stability lobe diagrams for milling process. The literature includes not only numerical [3] but also analytical [4,5] approaches for building stability lobe diagrams in milling. The common point of these studies is that all require the system dynamics information at the tool tip, which is expressed as the tool point FRF. The most common way of obtaining the tool point FRF is experimental modal analysis by impact testing at the tool tip, which is costly and time consuming since it should be repeated for every holder/tool changes during the applica-

tion. In order to minimize experimentation, Schmitz and Donaldson [6] implemented the receptance coupling theory of structural dynamics by using experimentally obtained spindle–holder dynamics and analytically obtained tool dynamics for the prediction of the FRF. The application of tool receptance coupling was improved in [7,8] and quite recently it was extended to the coupling of holder segments as well [9]. Ertürk et al. [10] developed an analytical model for the prediction of tool point FRF by using receptance coupling and structural modification techniques. Each segment of an individual component is modeled as a uniform (single-segment) free–free structurally damped beam, which are then coupled rigidly using their end point receptances for constructing a multi-segment beam representing the component. Instead of Euler–Bernoulli beam theory used in previous works, they used Timoshenko beam theory for increased accuracy. Due to the contact dynamics at the spindle–holder and holder–tool interfaces, these components are coupled elastically by using translational and rotational, springs and viscous dampers. Similarly, the bearing dynamics for the spindles are represented by viscously damped elastic members, which

*Corresponding author. Tel.: +90 312 210 2549; fax: +90 312 210 1266.
E-mail address: ozguven@metu.edu (H.N. Özgüven).

are included into the system using the structural modification technique suggested by Özgüven [11]. The components are coupled in order to obtain the end point receptance matrices of the assembly, and thus the tool point FRF which is required for the stability lobe diagrams. The gyroscopic effects, housing/machine dynamics and the work piece flexibility are neglected in the mathematical model used. Although simple spindle model is used, it is possible to include the mass of a motor or a pulley wheel integrated to spindle into the mathematical model.

Since it is the dynamic stiffness at the tool tip that shapes the stability lobe diagram of the assembly, it is important to understand the nature of tool dynamics and its sensitivity to system parameters for controlling the resulting stability lobe diagram in a favorable manner. Using the analytical model they developed, Ertürk et al. [12] studied the effects of bearing and interface parameters on the tool point FRF, from the results of which they suggested a new approach for the parametric identification of bearing, spindle–holder and holder–tool interface dynamics from experimental measurements [13]. They showed that the variations in connection flexibility strongly affect the modes appearing in the frequency range of interest.

In this paper, the effects of certain design and operational parameters on the tool point FRF, thus on the stability lobe diagram, are studied for typical spindle–holder–tool assemblies. The parameters of interest are divided into two groups as design and operational parameters. The first group includes parameters like spindle geometry, bearing stiffness values and bearing locations, which should be determined at the stage of spindle design. The second group consists of parameters which can be changed during the operation, such as holder/tool type and tool length or clamping torque.

2. Effects of design parameters on the FRF

In this section, the effects of typical spindle design parameters on the tool point FRF are studied. These parameters are determined by the machine tool builder at the design stage and they cannot be changed by the user.

2.1. Spindle geometry

Spindle geometry has a dominant effect on the frequency behavior of the whole assembly. Segment diameters and lengths are the parameters to be decided for optimizing the spindle dynamics. Consider the spindle (on bearings) shown in Fig. 1a and its tip point FRF. When a certain holder and a tool are connected to this spindle, the tool point FRF is obtained as shown in Fig. 1b. The assembly has typical dimensions, and average values obtained from the literature are used for interface and bearing parameters. The details of the model and the typical parameters are given in a recent paper [10]. Among the three modes captured in Fig. 1a, the first two modes are the rigid body modes and the third mode (at 1108 Hz) is the first elastic

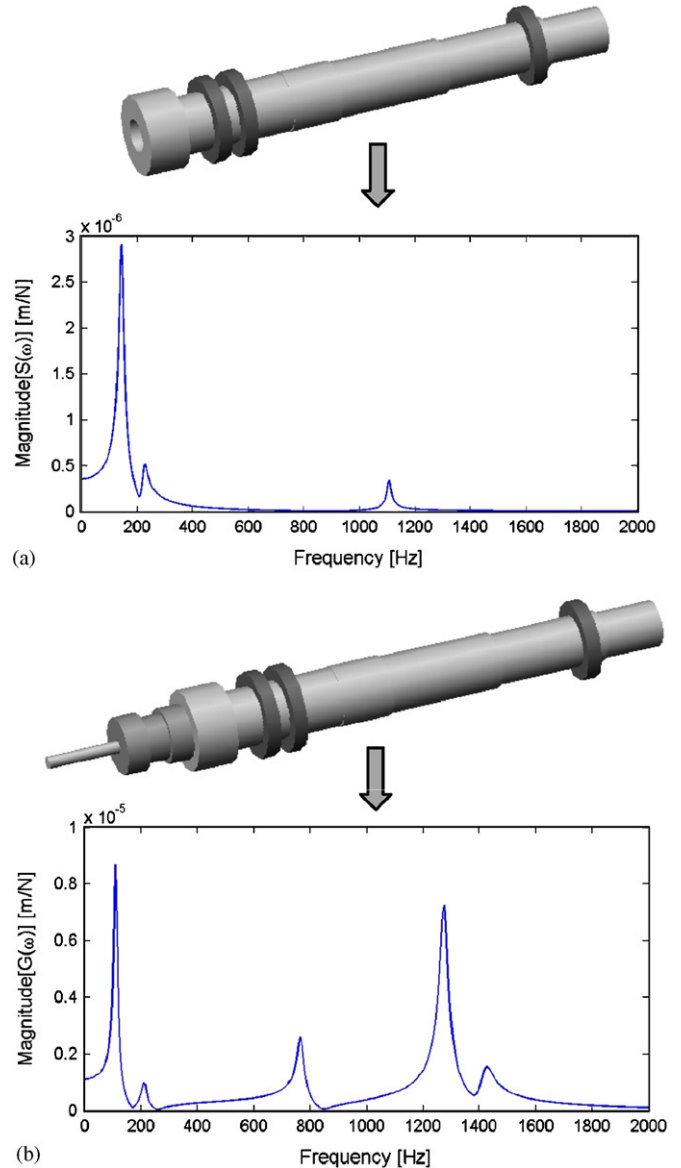


Fig. 1. (a) Spindle on bearings and its tip point FRF and (b) spindle–holder–tool assembly and its point FRF at the tool tip.

mode [12]. In the tool point FRF shown in Fig. 1b, three elastic modes are observed after the rigid body modes. Note that the addition of holder and tool slightly reduces the rigid body mode frequencies and increases their amplitudes considerably due to the increase in the total mass of the assembly.

Suppose that it is aimed to increase the first elastic mode of the individual spindle by changing the geometry of one of the segments (say, the one right at the center of the front and rear bearings) and observe the resulting variations in the tool point FRF. One can change either the diameter or the length of the segment for this purpose. If we aim to increase the frequency of the first elastic mode of the spindle, say to 1250 Hz, then it can be found from the model that the diameter should be increased from 61 to 81 mm. Fig. 2a shows the tip point FRF of the modified

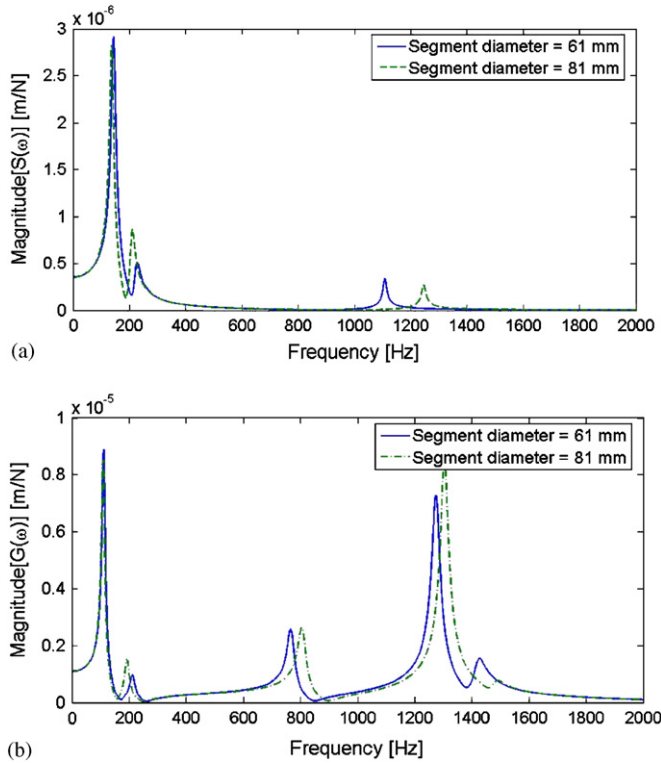


Fig. 2. Variations in the FRFs due to the change in segment diameter; (a) spindle tip point FRF (holder and tool are not inserted) and (b) tool point FRF of the assembly.

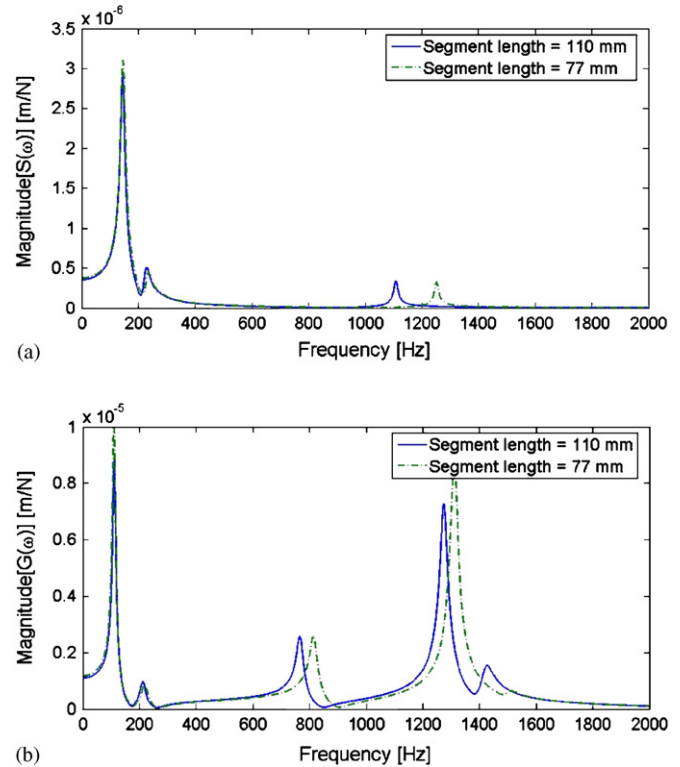


Fig. 3. Variations in the FRFs due to the change in segment length; (a) spindle tip point FRF (holder and tool are not inserted) and (b) tool point FRF of the assembly.

spindle (without holder and tool), together with that of the original one. The reflection of this variation on the tool point FRF is given in Fig. 2b.

The increase in the segment diameter increases the elastic mode frequencies of the spindle tip point FRF and also the elastic mode frequencies of the tool point FRF. The same effect can be realized by reducing the length of the segment of interest while its diameter is kept constant at 61 mm. The same frequency for the first elastic mode can be obtained if the segment length is decreased to 77 mm from its original length of 110 mm. The resulting FRFs are given in Fig. 3a and b for the spindle tip and at the tool tip, respectively.

Although similar variations in the elastic mode frequencies are obtained in Fig. 3 by changing the segment length instead of its diameter, the rigid body mode frequencies are not decreased but they are very slightly increased as oppose to the previous case, since the mass of the assembly is reduced. Segment inner diameters are also important parameters to be tuned for changing the dynamic stiffness of the spindle. It is important to note that, there is more than one way of obtaining the same effect as shown in the above example. Depending on the design problem (particularly on the size limitations) one should decide on changing the segment lengths or the diameters.

An interesting geometric design parameter for the spindle is its tail length, which is the free length behind the rear bearings. Consider Fig. 1b in which the tool point FRF of the assembly is given. As will be discussed in

Section 3.1, the dominant elastic mode seen at 1274 Hz is the tool mode and it is more sensitive to the variations in the tool length. When the spindle tail length is increased, it is expected that the elastic mode frequencies decrease. At this point, it is important to note that the first and the third elastic modes become more flexible with this variation, and for a certain tail length, the third elastic mode may catch the second elastic mode (the tool mode) and suppress its vibration amplitude. For the assembly given in Fig. 1b, if the tail length of the spindle is increased by 45 mm, the third elastic mode moves towards the tool mode and splits it into two separate modes with lower amplitudes at 1185 and 1374 Hz (Fig. 4). After this modification in the spindle geometry, the receptance magnitude at the original resonant frequency 1274 Hz is reduced to 3×10^{-7} from 7.3×10^{-6} m/N. This dynamic vibration absorber effect of the spindle tail can be utilized in the applications (where spindle is designed for specific holder–tool configurations) for suppressing the vibration amplitude of the tool mode.

2.2. Spindle bearings

It has recently been observed by Ertürk et al. [12] that the rigid body modes and the elastic modes of spindle–holder–tool assembly exhibit uncoupled behavior for the orders of magnitude of bearing and interface dynamic parameters identified in the literature [14]. The orders of magnitude identified in the referred work were in

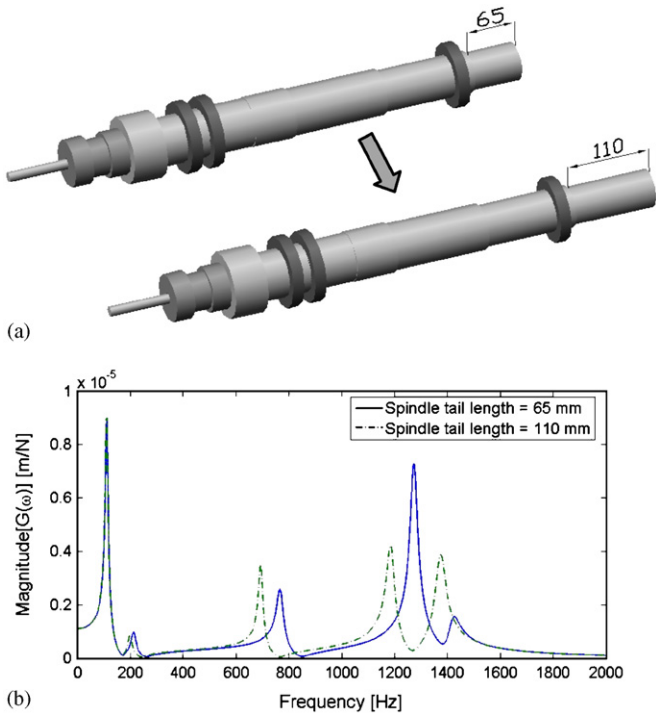


Fig. 4. (a) Modification in the tail length of the spindle and (b) the effect of the modification in the spindle tail length on the tool point FRF.

10^5 – 10^6 N/m. However, Cao and Altintas [15] obtained bearing stiffness values in the orders of magnitude of 10^7 – 10^8 N/m by using the bearing model they developed. As the literature includes a wide order of magnitude range for the bearing stiffness values, it is required to study the effects of bearing dynamics for each magnitude order to see the validity of the uncoupled behavior of rigid and elastic modes. In this section, it is shown that this uncoupled behavior depends highly on the orders of magnitude of bearing stiffness values. As it will be discussed below, the bearing locations can be important if their stiffness variations affect the elastic modes of the assembly.

Fig. 5a shows the effects of the bearing stiffness variation around the values used by Arakere et al. [14], which are in the orders of 10^5 – 10^6 N/m. As can be seen, the variations in the bearing stiffness values affect only the rigid body modes. These bearing stiffness values are so soft that even if the bearings are totally removed and the free-free assembly is considered, the elastic mode frequencies remain almost the same (Fig. 5b). It can be concluded that if the bearing preloads are so low that the bearing stiffness values are in the orders of 10^5 – 10^6 N/m, bearing locations are not important design parameters for controlling the elastic behavior of the assembly.

Bearing stiffness values start affecting the elastic modes of the FRF for the order of magnitude of 10^7 N/m (Fig. 6a). As can be seen from Fig. 6a, variations in the bearing stiffnesses alter the first elastic mode of the assembly, which is the spindle bending mode. The second elastic mode (the tool mode) is not affected from these variations. Fig. 6b shows the effects of the bearing stiffness

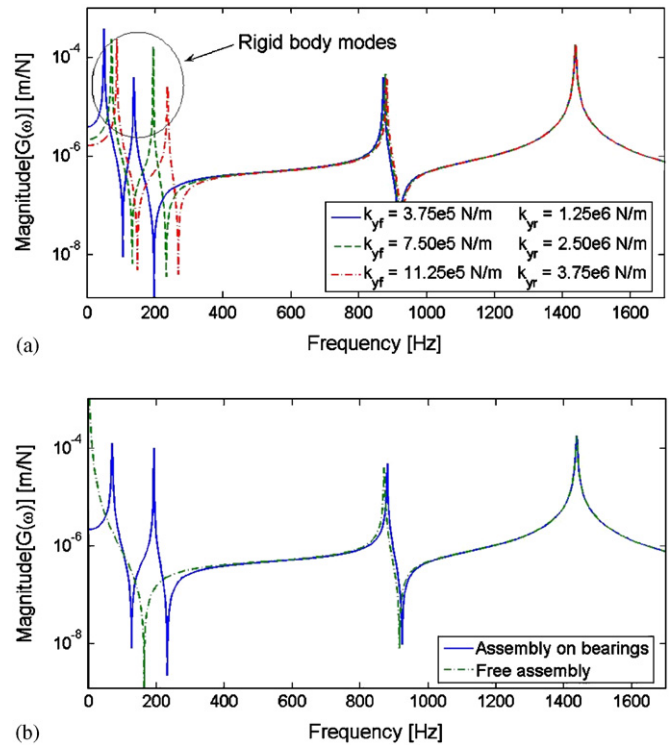


Fig. 5. (a) Effects of bearing stiffness (in the orders of 10^5 – 10^6 N/m) on the tool point FRF and (b) tool point FRFs of the bearing supported and free assembly.

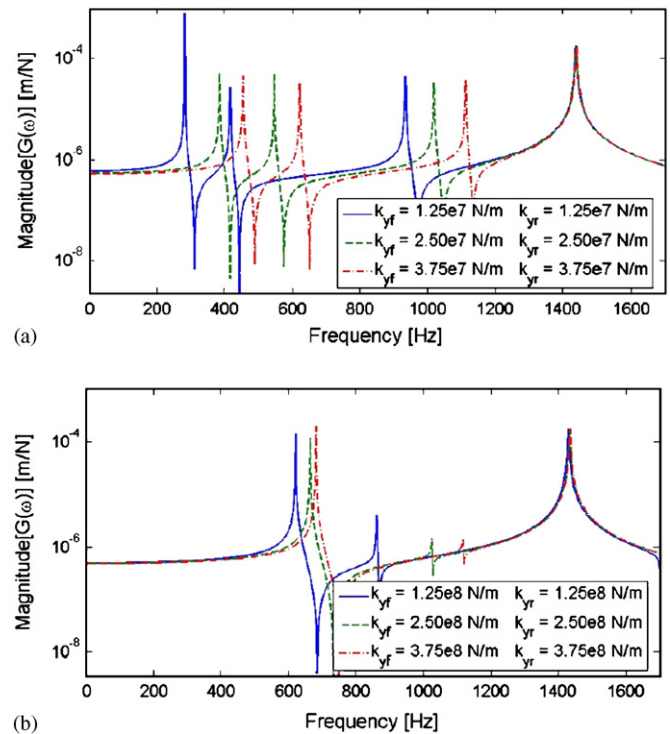


Fig. 6. (a) Effects of bearing stiffness (in the order of 10^7 N/m) on the tool point FRF and (b) effects of bearing stiffness (in the order of 10^8 N/m) on the tool point FRF.

on the FRF for the order of magnitude of 10^8 N/m. The second elastic mode is still unaffected from the variations in the bearing dynamics. It can be concluded that, in these orders of magnitude (10^7 – 10^8 N/m), bearing locations and the number of the bearings used affect the elastic modes (particularly the spindle bending modes) and they can be tuned for shaping the frequency response of the assembly.

3. Effects of operational parameters on the FRF

In machining operations, it may be required to change the tool and/or the holder for practical reasons. In addition, sometimes one may want to change the operational parameters such as the tool and the holder properties in order to modify the dynamic stiffness at the tip of the cutting tool. In this section, the effects of variations in these operational parameters on the tool point FRF are studied.

3.1. Tool geometry and holder–tool interface dynamics

In order to observe the effects of the tool overhang length on the FRF, the original tool overhang length (80 mm) of the assembly given in Fig. 1b is first increased to 90 mm and then to 100 mm by assuming that the connection dynamics is constant. As can be seen from Fig. 7a, the frequency of the second elastic mode is reduced by about 230 Hz for an increase of 20 mm in the tool overhang length. This mode is the tool controlled mode (or the tool mode) and as verified experimentally in Section 4.

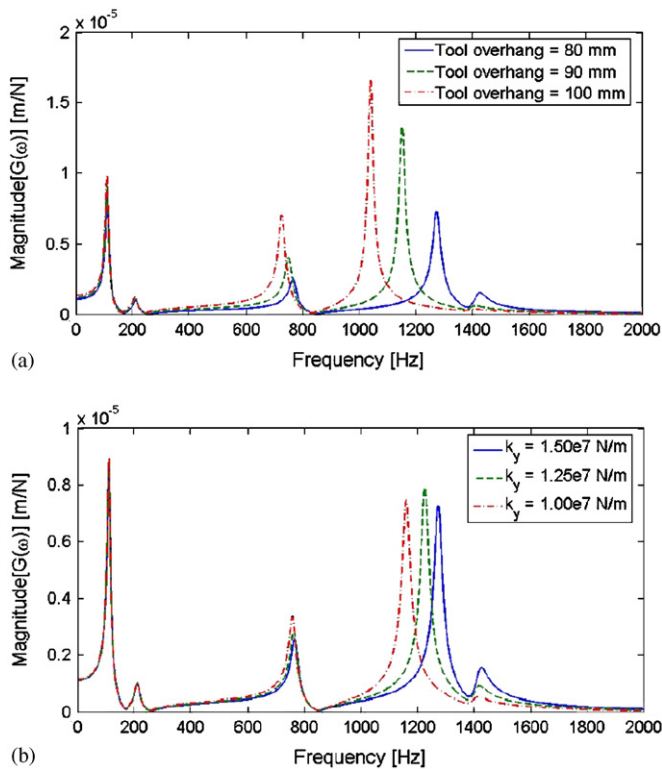


Fig. 7. (a) Effects of tool overhang length on the tool point FRF and (b) effects of holder–tool interface stiffness on the tool point FRF.

By changing the tool overhang length, its frequency can easily be altered in practical applications for modifying the tool point FRF and the stability lobe diagram of the assembly.

Investigation of the effects of tool diameter on the FRF results in the variations of the same mode. Therefore, when the tool is changed by another tool of a different diameter, one should expect important variations in the second elastic mode.

Ertürk et al. [12] have recently shown that the holder–tool contact dynamics, particularly the translational stiffness at this interface, controls the frequency of the second elastic mode in a typical assembly. With this information, in order to reduce the frequency of the tool mode, holder–tool interface translational stiffness is reduced and the variation given by Fig. 7b is obtained. It can be concluded that, if the translational stiffness of this connection can be modeled as a function of clamping torque and varied in a controllable manner, it is also possible to alter the frequency of the tool mode by just changing the clamping torque, without changing the tool overhang length. It should also be noted that the damping of holder–tool interface controls the peak of the tool mode [12] which can also be utilized in the same manner.

3.2. Holder geometry

Generally the parts of the holders inside the spindle are identical for different holder types but their segments outside the spindle differ from each other. For the assembly of interest (Fig. 1b), the diameters of each holder segment outside the spindle is increased by 10 mm in order to observe the variation in the FRF. The part of the holder outside the spindle is a very non-slender structure, which indeed acts as a mass. Thus, an increase in its segment diameters shifts the spindle modes to lower values due to the mass addition effect (Fig. 8a). Note that the tool mode is affected amplitude-wise without any variation in its frequency. However, when the length of the mid-segment of the holder is increased by 40 mm, in addition to the frequency shift of the spindle modes to lower values due to the mass addition effect, the frequency of the tool mode is also decreased due to an increase in the slenderness (therefore the flexibility) of the holder as can be seen in Fig. 8b.

4. Experimental verification

An SK40 type holder, in which a 4-teeth HSS tool of 110.7 mm length and 12 mm diameter is inserted, is assembled to the 5-axis machining center shown in Fig. 9a. Tool point FRF of the assembly is measured by impact test at the tool tip using a low mass accelerometer and an instrumented hammer. It is aimed in this section to predict the variations in the resulting FRF for different overhang lengths in order to improve chatter stability by tool tuning [16,17]. The predictions are compared with

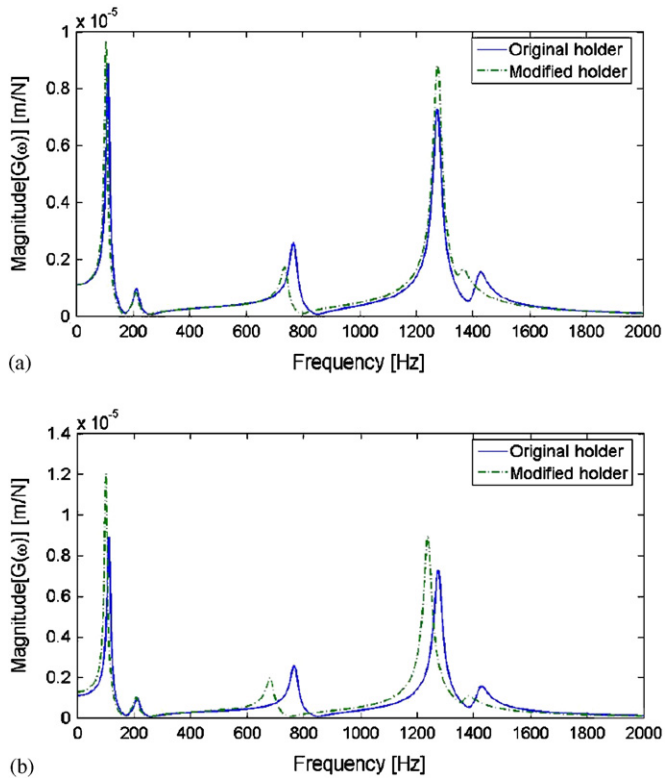


Fig. 8. (a) Effects of increase in the holder segment diameters on the tool point FRF and (b) effects of increase in the holder mid-segment length on the tool point FRF.

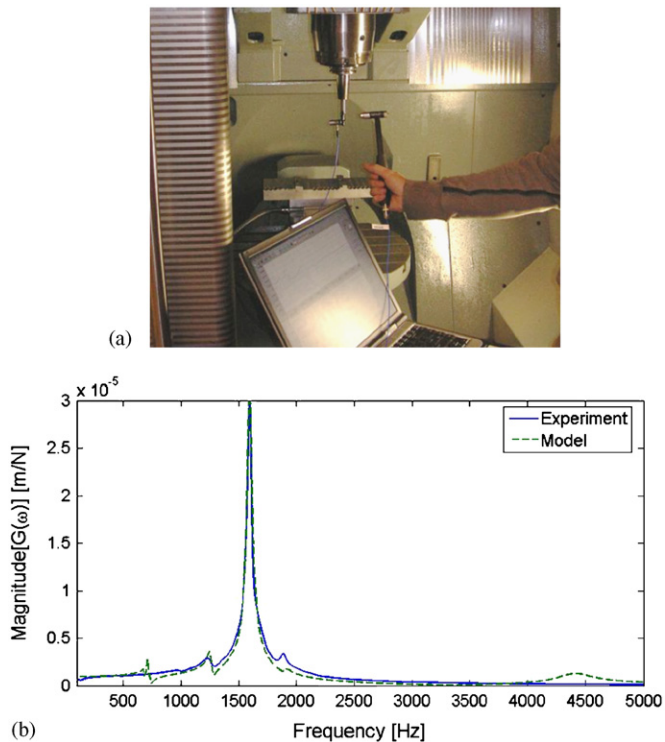


Fig. 9. (a) 5-axis machining center with the experimental modal analysis setup and (b) measured and predicted tool point FRF for the overhang length $L = 60$ mm.

experimental results for the verification of the approach employed. The translational interface dynamic parameters are identified by following the approach suggested in a recent work of the authors [12], using the experimental results for $L = 60$ mm. The average values given in the literature are used for the rotational dynamic parameters at spindle–holder and holder–tool connections, since the required FRF values are insensitive to these values as concluded in the above referred paper. The experimentally obtained tool point FRF and the model prediction for $L = 60$ mm are shown in Fig. 9b. The identified translational parameters at the spindle–holder and holder–tool interfaces are given in Table 1 along with the average rotational parameters used.

The dominant mode appearing at 1594 Hz is the tool mode as discussed previously. Therefore, its frequency can simply be altered by changing the overhang length of the tool. Overhang length of the tool is changed from 60 to 80 mm with an increment of 10 mm while keeping the clamping torque constant at 40 N.m. It is assumed that holder–tool interface dynamic parameters do not change with changing overhang length. Fig. 10a and b show the predicted and measured tool point FRFs for 70 and 80 mm tool overhang lengths, respectively. Note that, accurate knowledge of the variation in contact dynamics (especially damping) with tool overhang length would certainly improve the accuracy of the FRF predictions. That is, a mathematical model for contact stiffness and damping, or a methodology which provides this information for different clamping lengths, torques and tool types by using a limited set of experiments would yield more accurate theoretical results for FRF predictions.

As the overhang length of the tool is increased to 70 mm, the tool mode approaches to the small amplitude spindle mode seen around 1220 Hz, which slightly increases amplitude of the latter. Further increase in the tool overhang length (to 80 mm) brings the tool mode closer to the spindle mode and reduces the amplitude of the tool vibrations in a favorable manner as can be seen in Fig. 10b. The interaction between two modes reduces not only the frequency, but also the amplitude of vibrations. As a consequence, if this mode interaction can be realized in practical applications, higher depths of cut can be obtained at lower cutting speeds. In order to make use of this effect in practice, one should first identify the tool mode from the FRF and then alter its frequency towards a close and relatively stationary spindle mode by changing the tool overhang length until the mode is split and vibration amplitude is reduced.

The application of the presented method in the prediction of chatter stability has also been investigated. A series of tests have been conducted on an aluminum test piece. First, the cutting force coefficients were identified using milling tests and linear-edge force model [18]. The 4-teeth HSS end mill with 12 mm diameter and 30° helix angle mentioned above was used in down milling mode where the radial depth of cut was 3 mm. Different feed rates were

Table 1
The translational and the rotational dynamic parameters at the spindle–holder and holder–tool interfaces

Interface	Trans. stiffness (N/m)	Trans. damping (Ns/m)	Rot. stiffness (N m/rad)	Rot. damping (N m s/rad)
Spindle–holder	8.0×10^7	250	1.5×10^6	40
Holder–tool	7.5×10^6	32	1.5×10^6	40

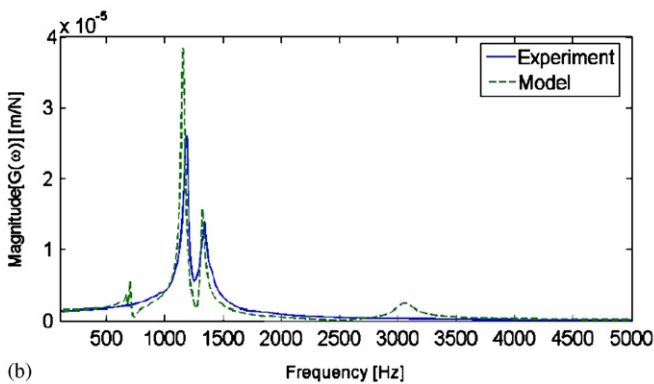
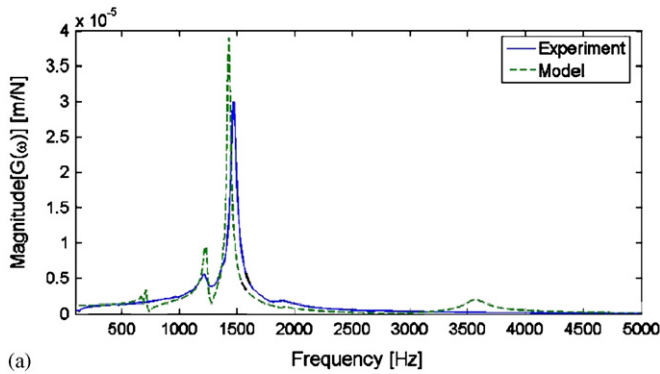


Fig. 10. Experimental and predicted tool point FRF; (a) 70 mm overhang length and (b) 80 mm overhang length.

used to identify the edge force coefficients: 0.05, 0.1, 0.15 and 0.2 mm/tooth. In order to observe the variation of the force coefficients with the cutting speed, the tests were repeated at 5000 and 10,000 rpm. Since usually constant force coefficients are used for the generation of stability diagrams, the average values of the coefficients were calculated after the edge forces were extracted. As a result, the tangential and the radial cutting force coefficients were obtained as $K_t = 550$ MPa and $K_r = 110$ MPa.

First of all, the stability diagram was generated for the case of 60 mm tool overhang length (Fig. 11) using the analytical milling stability model of Budak and Altintas [4,5]. The analytical model of Ertürk et al. [10] was employed for the prediction of tool point FRF where experimentally identified dynamic linear interface parameters and average rotational values from the literature were used at the tool–holder and holder–spindle interfaces. Predicted tool point FRF for 60 mm tool overhang length is given in Fig. 9b, where it was compared with the measured one. The experimentally obtained chatter stabi-

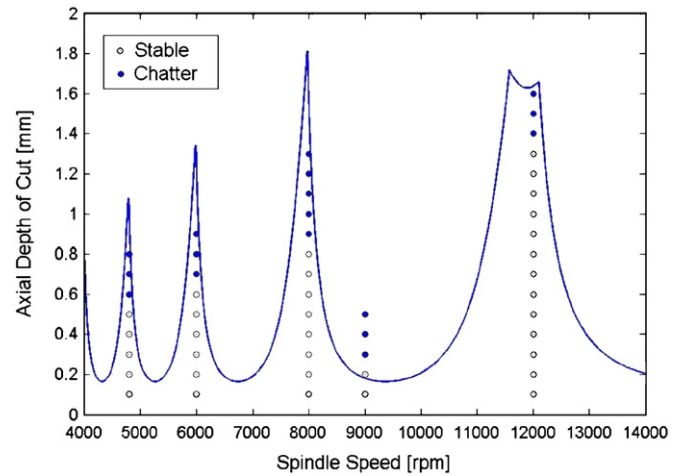


Fig. 11. Experimental and predicted stability limits for down milling of aluminum test piece using 60 mm tool overhang length and 3 mm radial depth.

lity limits at certain spindle speeds are also shown in Fig. 11. All cutting tests were performed on a high speed machining center (DMU 50evo). The instability condition was identified using the spectrum analysis of the sound measurements during cutting. Considering a wide speed range which results in variation in the force coefficients (the average values were used) and narrow stability pockets due to low damping, the agreement between the experimental and the analytical results can be considered as satisfactory.

As a second stability prediction application, the effect of the tool overhang length change on the stability diagram is considered. The tool overhang length may be changed due to operational requirements, or to modify the stability diagram to increase the stable depths at certain speeds. The model presented can be used for both cases. Fig. 12 shows stability diagram for 3 different tool overhang lengths: 60, 70 and 80 mm for the same cutting conditions used in the previous application. Again, the analytical method was used for the prediction of tool point FRF which was utilized in the analytical milling stability model together with the experimentally identified force coefficients for the generation of the diagrams. Note that due to the analytical FRF model, the prediction of the new FRFs for the new tool lengths is very fast and does not require additional testing. Fig. 12 shows that 60 mm tool overhang length results in very large stability lobe around 12,000 rpm. However, if the maximum spindle speed available on the spindle is less than this, say 10,000 rpm, then this lobe cannot be utilized. Moreover, this tool length results in a

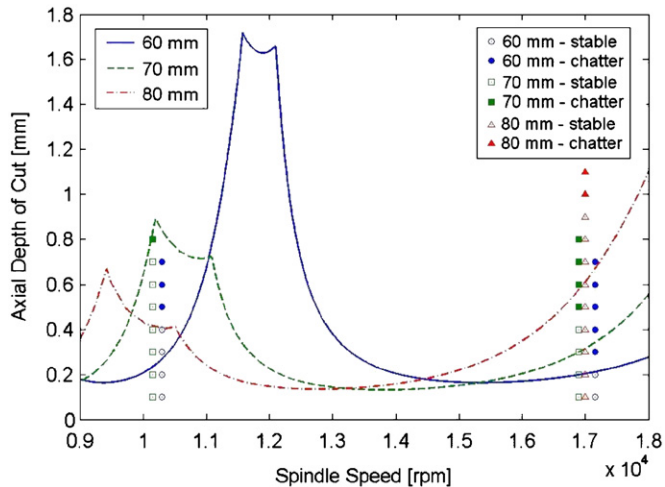


Fig. 12. Experimental and predicted stability limits for down milling of aluminum test piece using 60, 70 and 80 mm tool overhang lengths resulting in high stability lobes at different speed zones.

very low stability limit at around 10,000 rpm as shown in the diagram. Contrary to what one might expect intuitively, increasing the tool overhang length 10 to 70 mm produces a much higher stability pocket at this speed, and the depth of cut can be increased from 0.2 to 0.8 mm resulting in a substantial productivity gain. A similar problem arises if the process is to be carried out at a much higher spindle speed, say at 17000 rpm, if it is available on the machine. As it can be seen from the diagram, 60 mm tool overhang length again results in a very low stable depths at those speeds. However, unlike the previous case of 10,000 rpm, 70 mm tool overhang length does not produce much higher stability limits in this speed zone. In this case, increasing the tool overhang length another 10 mm to total of 80 mm produces much larger stability limits for those high speeds, resulting in about 3 folds amplification in the stable material removal rate. These predicted results are verified by chatter tests, and as shown in Fig. 12 the agreement between the experiments and the predictions is quite acceptable. Thus, it can be concluded that the integration of the analytical FRF and stability predictions can be a strong tool for a virtual machining environment where the stable and optimal conditions can be identified with minimal amount of testing.

5. Conclusions

In this paper, using the analytical model developed by the authors, the effects of certain design and operational parameters on the dynamics of spindle–holder–tool assembly are studied, and experimental demonstrations are given. The design parameters considered are the spindle geometry and bearing properties, whereas the operational parameters are the properties of the holder and the tool. In addition, the application of the model in chatter stability predictions is demonstrated with experimental verification.

Several important applications of the method have been demonstrated in the paper. It is shown that a desired variation in the resulting FRF can be obtained by proper selection of the diameter and/or the length of a spindle segment. For spindles, in addition to the segment geometries, the bearing locations can also be used for modifying the FRF. However, if the bearing preloads are low, the bearing locations may not have a significant effect on the dynamic stiffness of the assembly. On the other hand, if the stiffness values of the bearings are in the orders of 10^7 – 10^8 N/m, their locations can be altered for shaping the resulting FRF behavior. An interesting observation is that the tool mode of the assembly (the second elastic mode in this case) is not affected considerably from the variations in bearing dynamics. Although spindle configuration can only be changed by the machine manufacturer at the design stage, holder and tool properties are the most practical parameters which can be controlled by the user to alter the dynamics at the tool tip. It is observed that the geometry of the cutting tool controls the second elastic mode (the tool mode) of the typical assembly used in this study. Therefore, the frequency and the amplitude of this tool mode can be modified by changing the overhang length of the tool or the tool diameter. It is also observed that an increase in the diameters or the lengths of the holder segments reduces the frequencies of especially the spindle modes due to the mass addition effect since the parts of the holders outside the spindle are non-slender structures which act almost as pure mass in the system.

It is experimentally verified in this paper that the model developed by the authors can successfully be used for predicting stability lobe diagrams. It is also demonstrated in a 5-axis machining center that the model can be used to improve the chatter stability by changing operational parameters, such as the tool overhang length. As an example application, it is shown that while a 60 mm long tool overhang length provides a very large stability lobe at a certain cutting speed, at a lower speed where the same overhang length provides very low stability limits, a 10 mm longer length produces a high stability pocket, increasing the depth of cut 4 times. Interestingly, at a speed higher than the original speed, a further 10 mm increase in the tool overhang length results in 3 folds amplification in the stable material removal rate. These experimental observations are successfully predicted by the model developed. Therefore, it is concluded that the methodology presented in this paper can successfully be used in industrial processes for optimization of operational parameters in addition to its obvious application in virtual machining systems for chatter stability predictions with minimum amount of testing.

Acknowledgements

This work is supported by the Scientific and Technological Research Council of Turkey (TUBITAK) under project number 104M430, which is gratefully acknowledged.

Mr. Emre Özlü performed the chatter tests, which is also appreciated by the authors.

References

- [1] S.A. Tobias, W. Fishwick, The chatter of lathe tools under orthogonal cutting conditions, *Transactions of ASME* 80 (1958) 1079–1088.
- [2] J. Tlustý, M. Poláček, The stability of machine tools against self-excited vibrations in machining, in: *Proceedings of the ASME International Research in Production Engineering*, Pittsburgh, USA, 1963, pp. 465–474.
- [3] I. Minis, T. Yanushevsky, R. Tembo, R. Hocken, Analysis of linear and nonlinear chatter in milling, *Annals of the CIRP* 39 (1990) 459–462.
- [4] Y. Altintas, E. Budak, Analytical prediction of stability lobes in milling, *Annals of the CIRP* 44 (1995) 357–362.
- [5] E. Budak, Y. Altintas, Analytical prediction of chatter stability in milling—part I: general formulation; part II: application to common milling systems, *Transactions of ASME, Journal of Dynamic Systems, Measurement, and Control* 120 (1998) 22–36.
- [6] T. Schmitz, R. Donaldson, Predicting high-speed machining dynamics by substructure analysis, *Annals of the CIRP* 49 (1) (2000) 303–308.
- [7] S.S. Park, Y. Altintas, M. Movahhedy, Receptance coupling for end mills, *International Journal of Machine Tools and Manufacture* 43 (2003) 889–896.
- [8] E.B. Kivanc, E. Budak, Structural modeling of end mills for form error and stability analysis, *International Journal of Machine Tools and Manufacture* 44 (2004) 1151–1161.
- [9] T. Schmitz, G.S. Duncan, Three component receptance coupling substructure analysis for tool point dynamics prediction, *ASME Journal of Manufacturing Science and Engineering* 127 (2005) 781–790.
- [10] A. Ertürk, H.N. Özgüven, E. Budak, Analytical modeling of spindle–tool dynamics on machine tools using Timoshenko beam model and receptance coupling for the prediction of tool point FRF, *International Journal of Machine Tools and Manufacture*, 2006, in press, doi:10.1016/j.ijmachtools.2006.03.032.
- [11] H.N. Özgüven, A new method for harmonic response of non-proportionally damped structures using undamped modal data, *Journal of Sound and Vibration* 117 (1987) 313–328.
- [12] A. Ertürk, H.N. Özgüven, E. Budak, Effect analysis of bearing and interface dynamics on tool point FRF for chatter stability in machine tools by using a new analytical model for spindle–tool assemblies, *International Journal of Machine Tools and Manufacture*, 2006, in press, doi:10.1016/j.ijmachtools.2006.03.001.
- [13] E. Budak, A. Ertürk, H.N. Özgüven, A modeling approach for analysis and improvement of spindle–holder–tool assembly dynamics, *Annals of the CIRP* 56 (1) (2006) 369–372.
- [14] N. Arakere, T. Schmitz, C. Cheng, Rotor dynamic response of a high-speed machine tool spindle, in: *Proceedings of the 23rd International Modal Analysis Conference*, January 30–February 3, 2005, Orlando, FL (on CD).
- [15] Y. Cao, Y. Altintas, A general method for the modeling of spindle–bearing systems, *ASME Journal of Mechanical Design* 126 (2004) 1089–1104.
- [16] J. Tlustý, W. Zaton, F. Ismail, Stability lobes in milling, *Annals of the CIRP* 32 (1983) 309–313.
- [17] T. Schmitz, M. Davies, M. Kennedy, Tool point frequency response prediction for high-speed machining by RCSA, *Journal of Manufacturing Science and Engineering* 123 (2001) 700–707.
- [18] E. Budak, Y. Altintas, E.J.A. Armarego, Prediction of milling force coefficients from orthogonal cutting data, *Transactions ASME Journal of Manufacturing Science and Engineering* 118 (1996) 216–224.